THE PENNSYLVANIA STATE UNIVERSITY
SCHREYER HONORS COLLEGE

DEPARTMENT OF ASTRONOMY AND ASTROPHYSICS

SEARCHES FOR SUB-SOLAR MASS ULTRACOMPACT OBJECTS WITH ADVANCED LIGO

PHOEBE MCCLINCY
SPRING 2021

A thesis
submitted in partial fulfillment
of the requirements
for a baccalaureate degree
in Astronomy and Astrophysics
with honors in Astronomy and Astrophysics

Reviewed and approved* by the following:

Chad Hanna
Associate Professor of Physics, Astronomy and Astrophysics
Thesis Supervisor

Jane Charlton
Professor of Astronomy and Astrophysics
Honors Adviser

*Electronic Approvals on file in the Schreyer Honors College.

Abstract

There is increasing interest in sub-solar mass (SSM) black holes (BHs) regarding the possibility that they are a component of dark matter (DM), due to the limited knowledge regarding its composition. Dark matter is a mysterious type of matter that composes 85 percent of the matter in the universe. Little is known about the actual makeup of dark matter. Thus, it is hypothesized that black holes could account for a portion of the DM. Specifically, it is theorized that primordial black holes (PBHs) could account for DM. PBHs, which are BHs born in the Big Bang, have yet to be detected. The primordial black hole theory of dark matter may be tested by running a targeted search for SSM ultracompact objects using data collected by the Laser Interferometer Gravitational-wave Observatory (LIGO). LIGO uses gravitational waves (GW), ripples in the fabric of spacetime caused by energetic events in space, to discern information about systems of black holes and neutron stars in space. We define parameters that produce a search which simultaneously maximizes relative search sensitivity and minimizes computational cost. The dependence of template bank size on several parameter sets was tested, including the frequency range of the search, minimum mass, and spin. We determined that larger magnitudes of spin, wider frequency ranges, and smaller masses produce a larger template bank, and subsequently a higher computational cost. From this, we derived ideal parameters with which to conduct an Advanced LIGO search on O1 and O2 data for SSM binaries. A null result was produced from all searches; however, from our searches we are able to place constraints on the event rate and fraction of DM composed of SSM BHs, for BHs in the 0.2-1.0 $M_{\odot}$ range.

Table of Contents

List of Figures

List of Tables

Acknowledgements

Funding for this project was provided by by National Science Foundation grants PHY-2011865, OAC-1841598, and PHY-1454389, as well as Charles E. Kaufman Foundation (of the Pittsburgh Foundation) grants KA2019-105547 and KA2016-85224. The findings and conclusions included in this thesis do not necessarily reflect the view of these funding agencies. This project was additionally funded by the Pennsylvania State University Erickson Discovery Grant and the Pennsylvania State University Student Engagement Network Remote Innovation Grant. I also wish to acknowledge the Penn State Institute for Gravitation and the Cosmos for their support throughout my career.

I would like to thank my honors advisor, Dr. Jane Charlton, for academic support and for reading this thesis. I would like to thank my Millennium Scholars program coordinator Georjanne Rosa for her wonderful academic coaching and mentorship. I extend a multitude of thanks to my research advisor Dr. Chad Hanna, for believing in me from day one and for always pushing me to be the best student and scientist I can be. I am additionally grateful for Dr. Ryan Magee, without whose support and mentoring I would certainly not have made it this far. Thank you all.

Last but certainly not least, I thank my parents, for everything. This thesis is for you.

Chapter 1

Introduction

1.1 General Relativity and Gravitational Waves

In 1905, Albert Einstein published his theory of special relativity. Ten years later, in 1915, he published his theory of general relativity, which offered a glimpse into the mechanics of gravity. This theory of general relativity, also referred to as GR, describes gravity as an intrinsic property of the four-dimensional spacetime. When an object that has mass interacts with spacetime, a "warping" effect occurs in which the massive object bends the spacetime around it, as a bowling ball may do to a stretched-thin sheet of fabric.

While there were many tests of GR before it, a notable and applicable discovery was made by physicist Russell Alan Hulse and astrophysicist Joseph Hooton Taylor, Jr. in 1974. Known now as the Hulse-Taylor binary, the system identified by the scientists consisted of a neutron star and a pulsar. This marked the first-ever detection of a binary pulsar [1]. Over time the orbital period of the system has dwindled, as predicted by the theory of general relativity. Indeed, the rate of decay matches nearly perfectly with the predicted rate, as shown in Figure 1.1. This indicates the presence of gravitational radiation, resulting in a loss of mass and a decrease in the orbital period of the system. As far as tests of GR go, this particular system opened a new era of physics in its affirmation of the theory of GR.

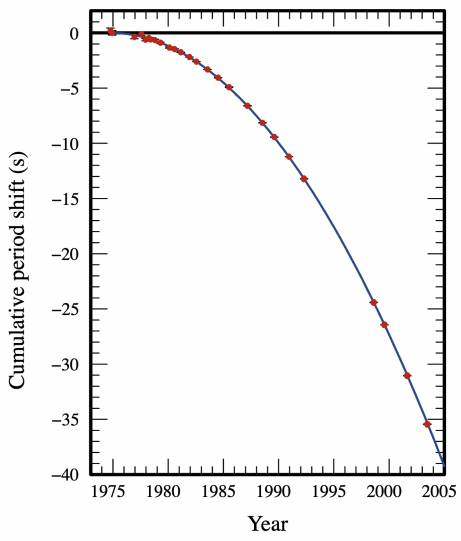

Figure 1.1: Cumulative period shift for the Hulse-Taylor binary over the years. It is evident that the observations, red, match nearly perfectly with theory, blue. These results are an ideal test of GR, and show that the predictions made by theory are correct. (Image credit: Wikipedia user Inductiveload, public domain.)

The very same gravitational radiation that caused the period shift of the Hulse-Taylor binary exists in systems across the universe. This radiation, also referred to as gravitational waves (GWs), can be thought of as ripples in the fabric of spacetime. GWs have the unique ability to shrink and expand the spacetime between masses. That is, GWs can bring masses closer or push them further apart in spacetime. This effect occurs on an extremely microscopic level, and can be measured using a quantity known as strain (h). Strain is represented as:

$$h = \frac{\Delta L}{L}, \tag{1.1}$$

where L represents the original distance between the masses in question, and ΔL represents the change in that distance. GWs, while able to induce this effect do so weakly, producing a strain of smaller than approximately 10^{-20}. GWs additionally propagate with two polarizations: plus (h_+) and cross ($h_\times$). Polarization is used to describe how the GW moves through spacetime. The plus polarization describes motion along the x and y axes, while the cross polarization describes motion along x and y axes rotated 45 degrees, shown in Figure (1.2).

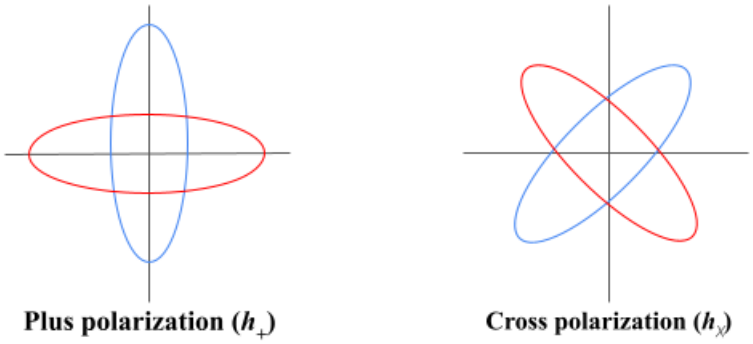

Figure 1.2: Plus polarization (left) vs. cross polarization (right) of a GW. The GW oscillates between the blue and red positions.

Implicit in the gravitational waveforms are fifteen parameters pertaining to the system in question, including but not limited to the primary (m_1) and secondary (m_2) masses, the luminosity distance to the binary (d_L), the inclination angle of the orbital angular momentum of the system with respect to the detector (i), as well as x, y, and z components of spin for each mass. Perhaps the most important of these fifteen parameters are the masses of each system component, as these parameters directly affect the strength of a GW signal. A more massive object produces a "louder" signal, and is therefore easier to detect from Earth. More often than not, when analyzing a GW signal, the quantity used to refer to mass is the chirp mass:

$$\mathcal{M} = \frac{(m_1 m_2)^{\frac{3}{5}}}{(m_1 + m_2)^{\frac{1}{5}}}. \tag{1.2}$$

In this regard, the plus and cross polarizations may be written in terms of the parameters of the GW signal (h) [2], including the chirp mass:

$$h_+ = 2\frac{\mathcal{M}}{d_L}(1 + cos^2 i)(\pi \mathcal{M} f)^{\frac{2}{3}} \cos(\Phi + \Psi), \tag{1.3}$$

and

$$h_\times = 4\frac{\mathcal{M}}{d_L} \cos i (\pi \mathcal{M} f)^{\frac{2}{3}} sin(\Phi + \Psi), \tag{1.4}$$

where $\mathcal{M}$ is chirp mass, d_L is luminosity distance, i is inclination angle, Ψ is the phase of the system, and

$$\Phi = -2\Big(\frac{T-t}{\mathcal{M}}\Big)^{\frac{5}{8}}, \tag{1.5}$$

$$f = \frac{1}{2\pi}\frac{\partial\Phi}{\partial t}. \tag{1.6}$$

Gravitational waves are emitted from a multitude of sources throughout the universe. One such category of GWs is known as continuous. These GWs are emitted from single celestial bodies, such as a neutron star. In order for these GWs to be released from a system, there must be a great deal of energy present in the system; i.e., the system must be spinning at a rapid rate. Moreover, the object of interest may not be spherically symmetric. That is, there must be some sort of imperfection on the surface of the object to result in the emission of continuous GWs. These GWs are expected to be much weaker than the ones LIGO has already detected [3].

A second category of GWs are known as stochastic, or "background" gravitational waves. It is believed that these GWs were released at the dawn of the universe, in the cataclysmic event known as the Big Bang. Since a great deal of time has passed between this event and the present, stochastic GWs are weak, and are thus very difficult to detect [4].

The third, and presently theoretical, type of GW is known as burst. These GWs have yet to be detected, and are currently unmodeled. This is due to the lack of knowledge surrounding the type of system that would emanate a burst GW. These GWs are expected to be very short in duration, and are difficult to predict; thus, physicists in search of these GWs must be prepared for anything [5].

The primary class of GWs that will be discussed in this paper are known as compact binary coalescence (CBC). CBC GWs are released from binary systems in space, such as a binary black hole (BBH) system, binary neutron star (BNS) system, or a neutron star-black hole (NSBH) system. As the two bodies in the system orbit each other, gravitational radiation is released in the form of mass loss. As a result of this, the two bodies grow closer and closer together in a phase known as inspiral. It is during this stage that the amplitude of the GW signal gradually increases. When the two bodies grow close enough, they collide and form a single massive body in a phase known as merger. During the merger phase, the amplitude of the GW signal sharply peaks. Finally, the new single body adjusts to its new state in a stage called ringdown, in which the amplitude of the GW signal gradually tapers off and flattens [6].

There are a plethora of different ways to detect gravitational waves. In particular there are two methods, known as interferometry and pulsar timing arrays (PTAs), that have proven to be useful and accurate. Interferometers operate by manipulating visible light to detect changes in their surroundings [7]. PTAs take advantage of the effects of general relativity, detecting GWs passing through by measuring changes in the rotational periods of known pulsars [8]. Currently, there are many scientific endeavors working on the feat of detecting GWs. In this paper, we will focus on the work of the Laser Interferometer Gravitational-wave Observatory.

1.2 History of LIGO

The Laser Interferometer Gravitational-wave Observatory (LIGO) is a ground-based interferometer operating out of the United States. In particular, there are two sites: one in Hanford, WA and another in Livingston, LA. Each site features a large-scale interferometer, modeled after the Michelson interferometer. As shown in Figure 1.3, these instruments work in a very precise way; a beam of laser light is directed towards a beam splitter, which divides the light into two perpendicular beams. These new beams travel down an arm of the interferometer, and at the end of the arm are reflected back up the arm to recombine and create destructive interference. That is, when the beams recombine, there is no visual pattern that appears. As mentioned previously, a marker of the presence of a GW is the expansion and contraction of spacetime. When a GW passes through the interferometers, the length of the interferometer's arms changes; in other words, the distance between the end points of each arm changes. This results in the appearance of a constructive interference pattern, indicating a GW. Each LIGO detector features arms of length 4 km (2.5 miles). Because the strain induced by gravitational waves is such a microscopic effect, the interferometer must be large enough to detect this miniscule change.

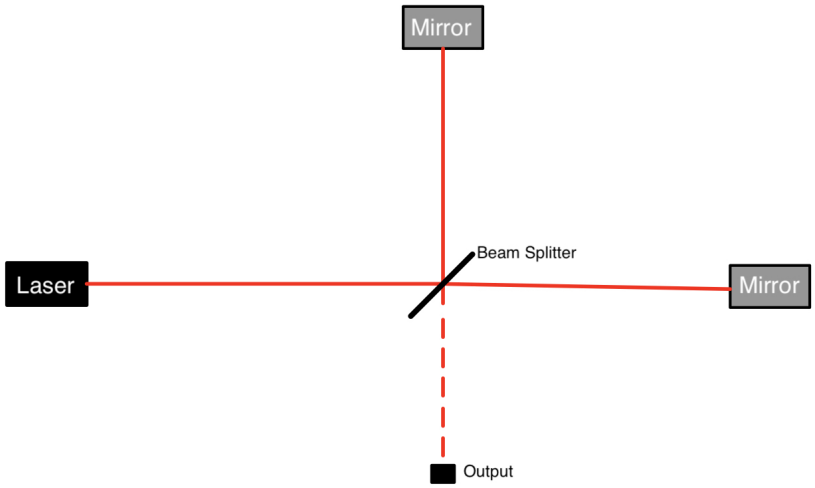

Figure 1.3: Diagram of a basic Michelson interferometer. The laser directs light at a beam splitter, which divides the light into two separate parts. These beams are directed down two arms, reflected back, and recombined to create a destructive (no GW) or constructive (GW) interference pattern.

LIGO is not the only ground-based interferometer in the world. LIGO works closely with the Virgo collaboration, which is based in Italy. The arms of the Virgo interferometer are only 3 km (1.86 miles) long. Moreover, LIGO assists in the operation of the GEO600 interferometer, located in Germany. Indicated by the name, the arms of this interferometer are 600 meters (1970 feet) long. LIGO additionally works with the Japanese KAGRA detector, whose arms are also 3 km (1.86 miles long). Beyond these ground-based interferometers, NASA plans to launch the Laser Interferometer Space Antenna (LISA), which will serve as a larger-scale interferometer in space.

Each of the ground-based interferometers mainly focuses on detecting gravitational waves from compact binary systems like BBHs, BNSes, and NSBHs. This is largely due to the frequency range

within which LIGO is able to search. LIGO was designed to be able to detect GW signals in the 10 Hz to 10 kHz range, but realistically are most sensitive between 10 Hz and 2 kHz, as shown in Figure 1.4. The main source of GWs in this frequency range is CBC systems.

Due to their incredibly sensitive nature, the LIGO interferometers are able to pick up on "signals" from other sources; this is referred to as noise. Many sources can cause noise, but one notable cause is gas trapped in the arms of the interferometer. Each arm is ideally a vacuum, free of any gas or other materials that may be blocking the laser light. However, in reality, this can only be achieved to a certain degree. There are still trace amounts of oxygen, nitrogen, and other gases trapped in the arms, each of which causes its own unique noise. Moreover, noise can be caused by quantum effects, as well as noise from the Earth itself. It is in part because of this noise that the LIGO interferometers are most sensitive in the 10 Hz to 2 kHz frequency range.

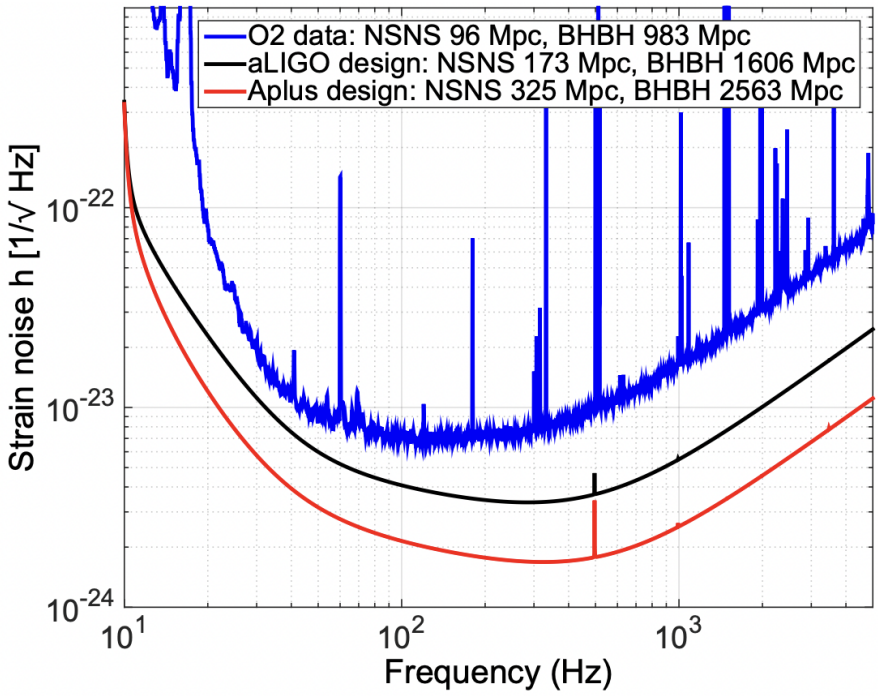

Figure 1.4: Sensitivity curves for LIGO throughout the years. The detectors reach a minimum (optimal) strain between frequency values of 20 Hz and 1 kHz. The detectors have yet to reach the design sensitivity for Advanced LIGO (black), but grow closer to this goal as improvements are made each year. As improvements are made, the detectors will move into the next phase, called A+ [9].

At present, LIGO has made tens of detections. The first detection made by LIGO, named GW150914 (for its detection date, 14 September 2015) [10], was comprised of two black holes of masses 36 $M_\odot$ and 29 $M_\odot$. This detection was incredibly groundbreaking, as it was the first detection made by the LIGO Scientific Collaboration in nearly 20 years of operation.

Shortly thereafter, another historic detection was made: GW170817, in which LIGO detected two neutron stars of approximate total mass 2.74 $M_\odot$ colliding in space. This detection was accompanied by a gamma-ray burst, GRB 170817A. The gamma-ray burst was detected by Fermi-GBM approximately 2 seconds after the LIGO detection was made. This gamma-ray burst detection,

well within the wheelhouse of multimessenger astronomy, was the first corroboration of a LIGO detection in history [11].

In 2019, history was once again made as LIGO detected what could be a neutron star-black hole (NSBH) merger. Candidate S190814bv, with over 99 percent probability of being a NSBH merger, had a primary mass greater than 5 $M_\odot$ and a secondary mass less than 3 $M_\odot$. This makes it a prime NSBH candidate. However, there is a possibility that this detection may be a "mass gap" detection, in which one component of the system would have a mass within the intermediate mass gap [12] (between approximately 2.0-5.0 $M_\odot$). The mass gap is further discussed in Section 1.3.

1.3 Primordial Black Holes and Dark Matter

One of the greatest unknowns in astronomy presently is dark matter (DM), which accounts for 85 percent of matter in the universe. However, its composition remains a mystery. At present, there has been no specific link to dark matter established. Little is known about the nature of dark matter, and as such it is often predicted that it may be connected to new physics that have yet to be discovered. There are many theories regarding the composition of dark matter, some of which LIGO may possibly be enabled to search for and find using gravitational waves.

In the entirety of its operation, LIGO has discovered tens of CBC systems with black hole and neutron star components. This has given shape to a mass distribution of black holes and neutron stars, as shown in Figure 1.5. Within this mass distribution, there exist three regions of scarcity: below 1 $M_\odot$ (sub-solar mass), between 2-5 $M_\odot$ (intermediate mass), and above appoximately 80 $M_\odot$. The intermediate mass gap is likely to exist due to the disparity between NS and BH masses. The smallest BHs exist around 5 $M_\odot$, and the largest NSes exist around 2 $M_\odot$. The highest mass gap exists due to pair-instability of high-mass BBHs. At high masses, these systems become unstable, causing an explosion that ejects a large amount, if not most, of the mass in the system. These largest systems tend to settle around the 80 $M_\odot$ region.

However, the sub-solar mass region is of particular interest, as it is not expected that a compact object like a black hole would form through traditional astrophysical processes in this mass range. Indeed, the smallest known black holes exist well above 1 $M_\odot$. It is hypothesized that a very specific type of black hole, known as a primordial black hole (PBH), may have formed in this region. These black holes are believed to have been formed in the Big Bang, and have yet to be detected. As they are theoretical in nature presently, much is speculated about the mass range in which these BHs would appear. Thus, it is entirely possible that these BHs exist in the region below 1 $M_\odot$. The origin of both PBHs and DM is up for much debate, and as such, it is additionally hypothesized that there may be a link between PBHs and DM. That is to say, PBHs could constitute some part of the mysterious dark matter.

In this thesis, we search data from LIGO's first and second observing runs (O1 and O2 respectively) for sub-solar mass ultracompact objects, specifically PBHs. If a detection were to be made in this mass region, it could be an indication of new physics, and could open the door to an entirely new area of study for astrophysicists. Additionally, these searches push the limits of LIGO's sensitivity and ability to search for low-mass compact objects.

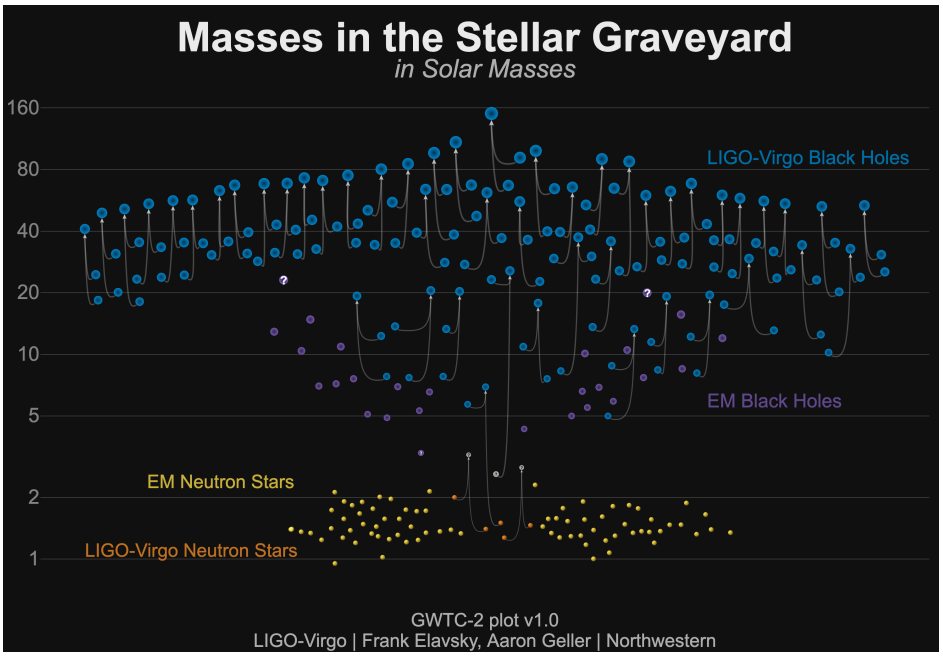

Figure 1.5: Mass distribution of neutron stars and black holes detected by LIGO, in solar masses. There are three regions of scarcity present; we are most interested in exploring the region below 1 $M_{\odot}$.

Chapter 2

Methods

2.1 Matched Filtering

In order to detect gravitational waves, LIGO uses a specific, thorough technique known as matched filtering. The signal-to-noise ratio (SNR) describes how likely the signal LIGO receives is to be an actual signal, and not noise. We may define the signal-to-noise ratio as:

$$\frac{S}{N} \equiv \frac{\langle \vec{h}(t), \vec{u}(t) \rangle}{\sqrt{\langle \vec{u}(t), \vec{u}(t) \rangle}}, \tag{2.1}$$

where $\vec{h}(t)$ is the raw waveform data from LIGO's detectors, and the $\vec{u}(t)$ is the template waveform we have predicted [13]. ($\vec{u}$, in actuality, is a function of the system parameters $\vec{\theta}$, but for simplicity we will call it $\vec{u}(t)$ only.) The inner product in this case, for two functions of time $a(t)$ and $b(t)$, is defined as:

$$\langle a, b \rangle = 2 \int_0^\infty df \frac{\tilde{a}^*(f)\tilde{b}(f) + \tilde{a}(f)\tilde{b}^*(f)}{S_h(f)}, \tag{2.2}$$

where

$$\tilde{a} = \int_{-\infty}^{\infty} dt e^{i2\pi ft} a(t), \tag{2.3}$$

and $S_h(f)$ is the detector's noise spectrum [14]. Equation (2.3) applies to $\tilde{b}(t)$, as well; this is the Fourier transform.

The process of matched filtering begins when the LIGO detectors gather data. Equations (1.3) and (1.4) enable LIGO to translate the physical strain the detector undergoes into a waveform. This waveform data can be compared to the templates ($\vec{u}$) we have predicted. These templates are predicted using predetermined models and equations that describe CBC systems and the GWs that they emit. The data is compared to thousands, and sometimes millions, of templates to determine if there is a match. The SNR is used to determine if there is a match or not [15]. A higher SNR indicates a better match; typically, LIGO uses an SNR threshold of 8 for a possible match.

If the template and the data are a match, the data moves on to further statistical analysis. The searches performed in this paper used the GstLAL analysis pipeline. Sometimes, data contains a phenomenon known as a glitch, which stems from environmental noise [16]. These glitches are able to imitate a real GW signal. In order to filter out glitches, the GstLAL pipeline checks the signal consistency. The check is performed by comparing the SNR at the glitch to the predicted SNR for a real signal. Often, glitches are very "loud" and can be ruled out [15].

After finding a match, the GstLAL pipeline determines if the data is consistent between all LIGO detectors. A log-likelihood ratio ($\mathcal{L}$) is then determined for each signal – this statistic describes how likely the signal is to be real. From this statistic, a quantitiy known as the false-alarm rate (FAR) is determined. The FAR describes the probability that a signal with log-likelihood ratio $\mathcal{L}$ would be detected from noise [15].

Given that the signal is strong in all of these categories, it will be considered a GW candidate.

2.2 Template Bank Generation

A template bank is a collection of the aforementioned templates. Certain CBC systems may be described by many templates; template banks collect these templates in one place for efficient analysis. Template banks are generated using computer programs written by LIGO members. These programs take as input the parameters of the search, i.e. masses, spins, and frequency range, and output a template bank from these parameters.

Each template bank is unique in size, dependent on the parameters that are input. These template banks contain hundreds of thousands of templates, and can sometimes contain millions of templates. For the searches performed in this paper, different parameter ranges and their effect on template bank size were analyzed, including mass range and frequency range, as well as the inclusion of spin. Template bank sizes are dependent on certain parameters of the system in question. Indeed, the template bank size ($\mathcal{N}$) is proportional to the minimum mass m_{min} [14]:

$$\mathcal{N} \propto m_{min}^{-2.7}. \tag{2.4}$$

When testing how changing f_{min} affected the template bank size, minimum mass was kept to 0.19 $M_{\odot}$, maximum mass was kept to 2.0 $M_{\odot}$, and spin was kept to 0. Three different sets of frequency ranges were tested, with each of the sets corresponding to a maximum frequency of either 512 Hz, 1024 Hz, or 2048 Hz. Each maximum frequency was tested with each minimum frequency (40 Hz, 55 Hz, and 70 Hz):

f_{min} **(Hz)**	f_{max} **(Hz)**	**Template Bank Size**
40.0	512.0	527632
55.0	512.0	222946
70.0	512.0	113903
40.0	1024.0	471416
55.0	1024.0	238035
70.0	1024.0	128445
40.0	2048.0	478633
55.0	2048.0	244276
70.0	2048.0	135040

Table 2.1: Effects of altering f_{min} for searches

For all values of f_{max}, the template bank size decreases as f_{min} increased, meaning that the template bank size decreased as the size of the frequency range decreased. This demonstrates an inverse relationship between f_{min} and template bank size.

These data were also used to test how changing f_{max} affected the template bank size. It was found that for f_{min} = 40 Hz, template bank size decreased between f_{max} = 512 Hz and f_{max} = 1024 Hz, but increased between f_{max} = 1024 Hz and f_{max} = 2048 Hz. For both f_{min} = 55 Hz and 70 Hz, the template bank size steadily increased as the f_{max} value increased, showing a direct relationship between f_{max} and the template bank size.

From these data, it is clear that a larger frequency range resulted in a larger template bank size, and subsequently a larger computational cost. This is supported by Figure 2.1, in which a smaller f_{min} results in a larger computational cost.

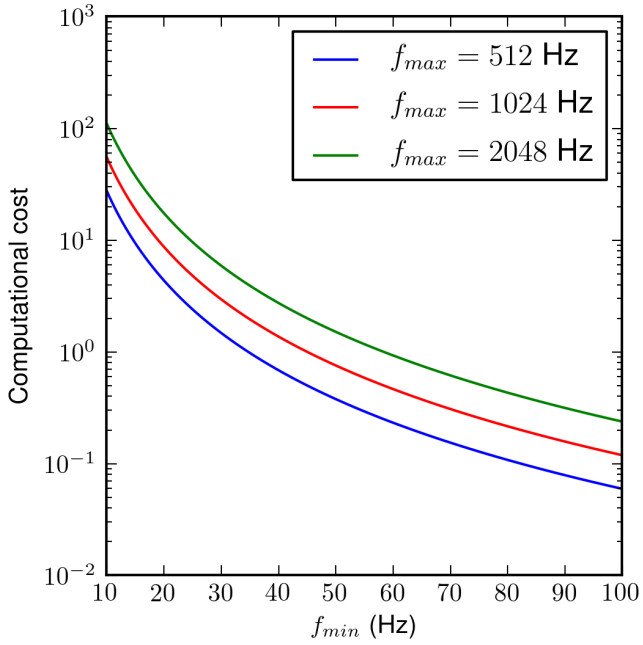

Figure 2.1: Computational cost, as affected by varying f_{min}, for fixed values of f_{max} including 512 Hz, 1024 Hz, and 2048 Hz.

When testing how changing m_{min} would affect template bank size, minimum frequency was set to 70 Hz, maximum frequency was set to 512 Hz, spin was set to 0, and maximum mass was set to 2.0 $M_{\odot}$.

$M_{min}(\mathbf{M}_{\odot})$	**Template Bank Size**
0.10	526684
0.15	202849

Table 2.2: Effects of altering M_{min} for searches

As minimum mass increases, the template bank size decreases, meaning that as the range of masses becomes smaller, so does the template bank size. This indicates an inverse relationship between m_{min} and template bank size. From these data, it can be concluded that there is a direct relationship between the size of the range of masses and template bank size, i.e. a larger range of masses results in a larger template bank.

When testing how changing spin would affect template bank size, two separate sets were tested. For the first set of data, minimum mass was set to 0.05 $M_{\odot}$, maximum mass was set to 0.20 $M_{\odot}$, minimum frequency was set to 100 Hz, and maximum frequency was set to 512 Hz. Minimum spin was kept at 0, with maximum spin varying.

Spin	Template Bank Size
0.10	414718
0.20	643470
0.30	862932

Table 2.3: Effects of altering spin for searches, M_{min} = 0.05 $M_{\odot}$

For the second set of data, minimum mass was set to 0.19 $M_{\odot}$, maximum mass was set to 2.0 $M_{\odot}$, minimum frequency was set to 70 Hz, and maximum frequency was set to 512 Hz. Minimum spin was kept at 0, with maximum spin varying once again.

Spin	Template Bank Size
0.10	150945
0.20	195511
0.30	242095
0.50	329010
0.70	414625

Table 2.4: Effects of altering spin for searches, M_{min} = 0.19 $M_{\odot}$

From both sets of data, it can be concluded that as maximum spin is increased, template bank size also increases, indicating a direct relationship between the template bank size and the size of the spin range. That is, a larger range of spins will produce a larger template bank.

We performed this analysis on the varying of parameters in order to optimize the computational cost of this project. As template banks become larger, the computational power required to search through the data increases. With more templates, there is more data to sift through, resulting in more time and energy required of LIGO's computational resources. Therefore, it is important to conduct a search that is simultaneously thorough and the least computationally-costly possible. We determined that the best parameters to use for our search were a frequency range of 45-1024 Hz, and a mass range of 0.19-2.0 $M_{\odot}$. Spin was not factored into the O1 search, but was included in the O2 search.

Chapter 3

Interpretation of Results

3.1 Analysis of O1 and O2 Data

Using the data collected during LIGO's first observing run, dated 12 September 2015 to 19 January 2016, a search was performed in the mass range 0.19-1.0 $M_\odot$, and the frequency range 45-1024 Hz. It was assumed that high-mass-ratio systems could occur. Additionally, binaries in this search did not have spin. When unusable data are discarded, this amounts to an analysis of 48.16 days of data. Using the matched filtering methods detailed in section 2.1 above, these data were searched for primordial black hole candidates. A total of 500,332 templates were searched; the search yielded a null result, with no viable GW candidates found in the 0.19-1.0 $M_\odot$ region [17].

The search then moved on to LIGO's second observing run, analyzing data dated 30 November 2016 to 25 August 2017. When unusable data are discared, this amounts to an analysis of 117.53 days of data. Again, the matched filtering methods detailed in section 2.1 were used to conduct this search. The search was performed in the frequency range 45-1024 Hz, and the mass range 0.19-2.0 $M_\odot$, with total masses ranging from 0.4-4.0 $M_\odot$. Unlike the O1 search, spin was indeed factored into the O2 search, with magnitude up to 0.1. After searching through 992,461 templates, a null result was again found [18].

3.2 Discussion of Results

As discussed in Section 3.1, a null result was obtained for both the O1 [17] and the O2 [18] sub-solar mass ultracompact object searches. However, this provides much valuable information about potential sub-solar mass ultracompact objects.

From a null result such as those in O1 and O2, the binary merger rate for sub-solar mass ultracompact objects may be constrained. In the case of the O1 search, the binary merger rate for SSM UCOs was constrained for nine different mass distributions between 0.2-1.0 $M_\odot$. These mass distributions were assumed to be for equal-mass binaries with zero spin. These constraints were derived by running a simulated search similar to the O1 SSM UCO search, in which known signals were injected into data and recovered. From this practice, the detection efficiency $\epsilon_i(r)$ can be calculated. From the efficiency, the volume-time can be calculated as such:

$$\langle VT \rangle_i = T \int 4\pi r^2 \epsilon_i(r) dr. \tag{3.1}$$

The volume-time describes the amount of spacetime that can be searched – in this case, via a search similar to the one conducted on O1 data. For the O1 search, T is equal to the elapsed time of O1 data, 48.16 days. Finally, the merger rate to 90 percent confidence, can be modeled as:

$$\mathcal{R}_{90,i} = \frac{2.3}{\langle VT \rangle_i}. \tag{3.2}$$

This equation represents an upper limit on the merger rate [17].

Similarly, the merger rate was derived for the O2 search. The O2 search results in a merger rate constraint that is approximately 3 times tighter than the constraint derived from the O1 search. This improved constraint is a result of not only increased LIGO overall sensitivity, but also the

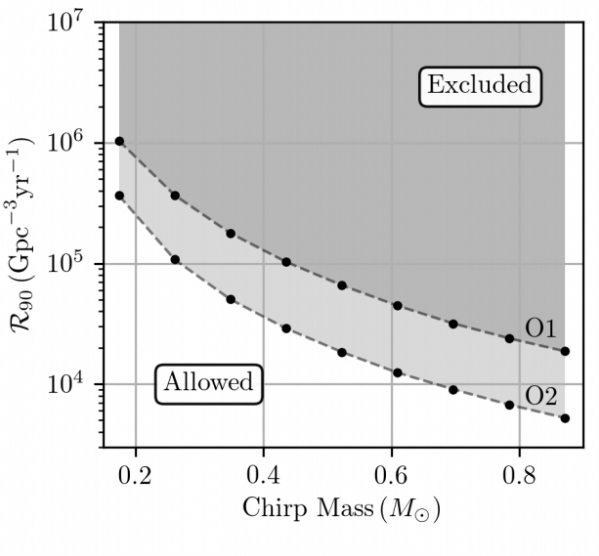

Figure 3.1: Merger rate constraints to 90 percent confidence for mass range 0.2-1.0 $M_\odot$. As displayed in the figure, the results from the O2 search are approximately 3 times tighter than those derived from the O1 search. The gray shaded region represents the excluded area. [18]

increase in the amount of data analyzed (117.53 days of data analyzed for O2, compared to 48.16 days of data for O1) [18]. The constraints derived for both searches are displayed in Figure 3.1.

Moreover, the null result yielded from the O1 and O2 searches lends insight on the fraction of dark matter allowed to be composed of primordial black holes. This quantity will be denoted f. Constraints on f were derived as a result of the constraints on $\mathcal{R}$. This is done using the equation

$$\mathcal{R} = n_{BH}\frac{dP}{dt}, \tag{3.3}$$

in which $\frac{dP}{dt}$ is a function of f [17]. The results for the O1 search are shown in Figure 3.2, and the results for the O2 search are shown in Figure 3.3.

3.3 Implications of Results

While on the surface it may not seem so, a null result is not inherently a bad result. Indeed, for these searches, a more defined search area has been derived in the form of both merger rate constraints and constraints on the fraction of dark matter allowed to be composed of PBHs.

The binary merger rate lends insight on the amount of PBHs/SSM UCOs that exist in the universe. By deriving constraints on the binary merger rate, we have derived constraints on the amount of SSM UCOs in the universe. In regard to the constraints on f, an entire region of f has been ruled out, and future searches can build on these findings. That is, with every null result, these constraints will become tighter and, in a sense, more accurate as more data are collected and analyzed.

Furthermore, if in future searches a viable candidate were to be found, the O1 and O2 searches

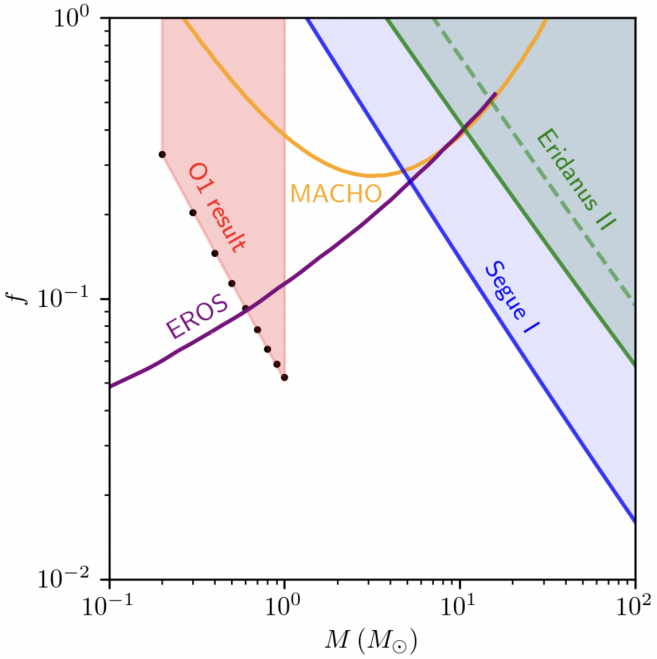

Figure 3.2: Fraction of dark matter f allowed to be composed of PBHs of a certain mass M. The constraints derived in the LIGO O1 search are shown in red. Other results from other surveys are additionally shown. LIGO produces a more constraining result than the MACHO survey in the 0.1-1.0 $M_\odot$ mass range, as well as a more constraining result than the EROS survey in the 0.7-1.0 $M_\odot$ range. [17]

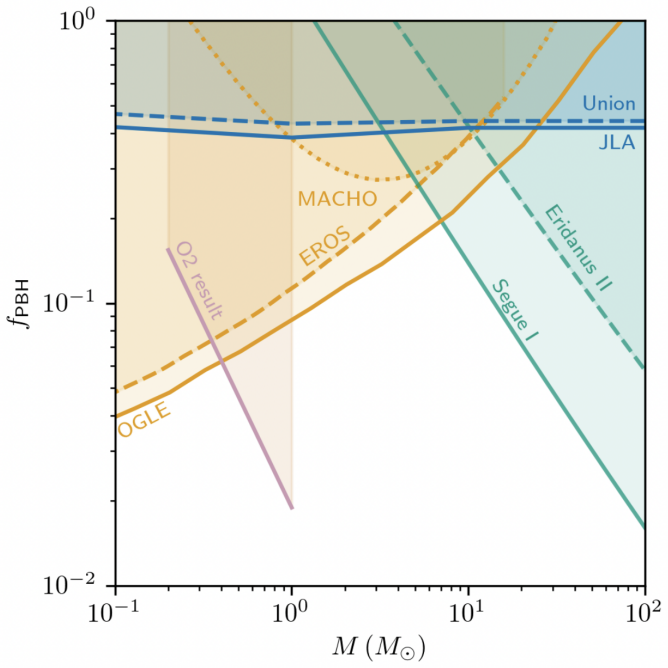

Figure 3.3: Fraction of dark matter f allowed to be composed of PBHs of a certain mass M. The constraints derived in the LIGO O2 search are shown in pink. Other results from microlensing surveys, supernova lensing surveys, and dwarf galaxies with unknown dark matter components, are also shown in orange, blue, and cyan respectively. In the 0.1-1.0 $M_\odot$ mass range, LIGO produces the most constraining result for the model used in the O2 search. [18]

have allowed us to develop methods for detecting such a candidate. With each search, these methods become more refined.

Chapter 4

Conclusion

4.1 Summary

In summary, we have conducted searches through LIGO's O1, O2, and O3 data in search of sub-solar mass ultracompact objects, specifically primordial black holes. In order to carry out these searches, we were required to do a computational analysis on the searches, i.e. determine how computationally costly the searches would be. It was found that larger frequency ranges, larger mass ranges (lower minimum mass), and the inclusion of spin in the searches produced a more computationally costly search. The searches were carried out between 45-1024 Hz, and between 0.2-1.0 $M_{\odot}$. Spin was not included in the O1 searches, but was included in some of the O2 and O3 searches.

These searches have yielded a null result, and no viable gravitational wave candidates were found in any of the searches. However, we are able to use this information to place constraints on the binary merger rate for primordial black holes, as well as constraints on the fraction of dark matter allowed to be composed of primordial black holes. These results have provided us with a general idea of the amount of PBHs or SSM ultracompact objects that may exist in the universe. The searches through LIGO's O2 data have improved on the constraints derived from the O1 searches, and it is expected that the results of the O3 search will improve on the constraints derived from the O2 search. It is important to note that spin was not factored into the calculation of these constraints for O1, but it was for O2; that is, the waveforms used to derive these constraints were assumed to be from systems with no spin in the O1 searches.

4.2 Future Prospects and Implications

There are many areas for improvement and further work moving forward with searching for SSM ultracompact objects. Already the search through O2 data has expanded on the search through O1 data; the search area included systems with spin, and the constraints derived from the O2 data included more generalized populations of SSM ultracompact objects. Using the constraints we have derived, paired with constraints that already existed, we have potentially provided a thorough constraint on particulate dark matter, as well as nuclear interaction cross section. It is in this very manner that future searches will allow us to be informed about the nature of dark matter.

As shown in Figure 4.1, the constraints on the fraction of dark matter allowed to be composed of primordial black holes were expected to improve by two orders of magnitude, given another null result from the searches we have recently conducted. In future searches, this constraint will improve even more than shown here, as more data is amassed to search through and LIGO's sensitivity improves. As LIGO's sensitivity improves, we will be able to "see" further into the universe, picking up binaries with smaller component masses and binaries that are further away from our detectors. This will provide us with the opportunity to place tighter constraints not only on the fraction of DM allowed to be composed of PBHs, but also the binary merger rate for PBHs. The merger rate allows us to picture how many PBHs may exist in space at all; provided with more data and higher sensitivity, the constaints we place on the merger rate will be more accurate and will allow us to know an abundance of PBHs that is closer to the truth. These constraints in turn provide us with a smaller search area for PBHs.

In future searches, we can additionally include spin as a factor in calculating the waveforms with which we search. While adding spin as a parameter in these searches does indeed increase the

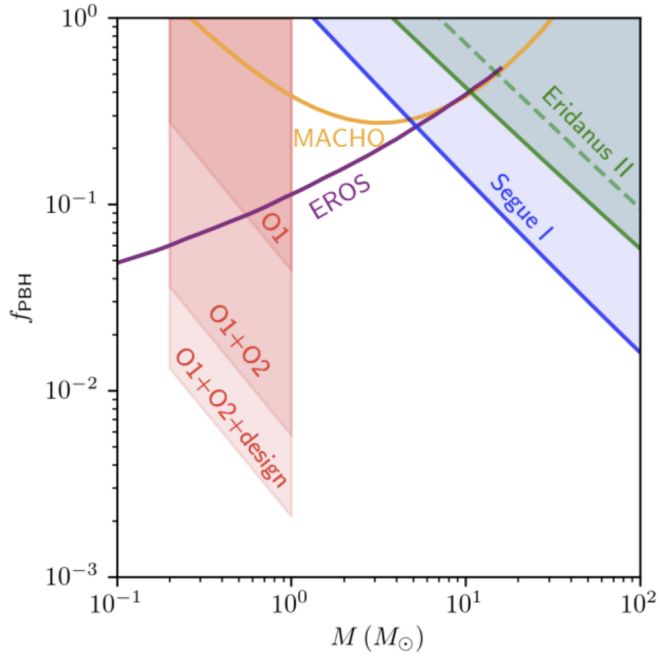

Figure 4.1: With mass on the x-axis ($M_\odot$) and fraction of DM allowed to be composed of PBHs on the y-axis, this plot shows the constraints derived from our searches, as shown in the figure above. LIGO's results are shown in pink; this particular plot shows the projected improvement in constraints on f between the O2 and O3 searches. Given a null result, the O3 constraints were expected to improve upon the O1 and O2 constraints by approximately two orders of magnitude.

computational cost, the computational power of LIGO's resources is improving each day. In the future, when these computational resources have reached a certain strength, we may include spin in all of our searches. Spin is a higher-order effect in GW signals; therefore, by including spin in our searches, we may be able to derive more information about detected binaries from the signals we obtain. This includes determining mechanisms of formation for PBHs and SSM ultracompact objects in general.

Bibliography

[1] R. A. Hulse and J. H. Taylor, "Discovery of a pulsar in a binary system," *The Astrophysical Journal*, vol. 195, pp. L51–L53, 1975.

[2] L. S. Finn and D. F. Chernoff, "Observing binary inspiral in gravitational radiation: One interferometer," *Physical Review D*, vol. 47, no. 6, p. 2198, 1993.

[3] K. Riles, "Recent searches for continuous gravitational waves," *Modern Physics Letters A*, vol. 32, no. 39, p. 1730035, 2017.

[4] B. Abbott, R. Abbott, R. Adhikari, A. Ageev, B. Allen, R. Amin, S. Anderson, W. Anderson, M. Araya, H. Armandula, *et al.*, "Analysis of first ligo science data for stochastic gravitational waves," *Physical Review D*, vol. 69, no. 12, p. 122004, 2004.

[5] M. Ando, K. Arai, S. Nagano, R. Takahashi, S. Sato, D. Tatsumi, Y. Tsunesada, N. Kanda, S. Kawamura, P. Beyersdorf, *et al.*, "Analysis methods for burst gravitational waves with tama data," *Classical and Quantum Gravity*, vol. 21, no. 20, p. S1679, 2004.

[6] I. Mandel and R. O'Shaughnessy, "Compact binary coalescences in the band of ground-based gravitational-wave detectors," *Classical and Quantum Gravity*, vol. 27, no. 11, p. 114007, 2010.

[7] B. Abbott, R. Abbott, R. Adhikari, P. Ajith, B. Allen, G. Allen, R. Amin, S. Anderson, W. Anderson, M. Arain, *et al.*, "Ligo: the laser interferometer gravitational-wave observatory," *Reports on Progress in Physics*, vol. 72, no. 7, p. 076901, 2009.

[8] R. Manchester, "The international pulsar timing array," *Classical and Quantum Gravity*, vol. 30, no. 22, p. 224010, 2013.

[9] L. Barsotti, L. McCuller, M. Evans, and P. Fritschel, "The a+ design curve," *LIGO DCC*, 2018.

[10] B. P. Abbott, R. Abbott, T. Abbott, M. Abernathy, F. Acernese, K. Ackley, C. Adams, T. Adams, P. Addesso, R. Adhikari, *et al.*, "Properties of the binary black hole merger gw150914," *Physical review letters*, vol. 116, no. 24, p. 241102, 2016.

[11] B. P. Abbott, R. Abbott, T. Abbott, F. Acernese, K. Ackley, C. Adams, T. Adams, P. Addesso, R. Adhikari, V. Adya, *et al.*, "Gw170817: observation of gravitational waves from a binary neutron star inspiral," *Physical Review Letters*, vol. 119, no. 16, p. 161101, 2017.

[12] H. Wei and M. Feng, "The possible electromagnetic counterparts of the first high-probability nsbh merger ligo/virgo s190814bv," *Communications in Theoretical Physics*, vol. 72, no. 6, p. 065401, 2020.

[13] C. W. Helstrom, *Statistical theory of signal detection: international series of monographs in electronics and instrumentation*, vol. 9. Elsevier, 2013.

[14] B. J. Owen, "Search templates for gravitational waves from inspiraling binaries: Choice of template spacing," *Physical Review D*, vol. 53, no. 12, p. 6749, 1996.

[15] S. Sachdev, S. Caudill, H. Fong, R. K. Lo, C. Messick, D. Mukherjee, R. Magee, L. Tsukada, K. Blackburn, P. Brady, *et al.*, "The gstlal search analysis methods for compact binary mergers in advanced ligo's second and advanced virgo's first observing runs," *arXiv preprint arXiv:1901.08580*, 2019.

[16] R. E. Colgan, K. R. Corley, Y. Lau, I. Bartos, J. N. Wright, Z. Márka, and S. Márka, "Efficient gravitational-wave glitch identification from environmental data through machine learning," *Physical Review D*, vol. 101, no. 10, p. 102003, 2020.

[17] B. Abbott, R. Abbott, T. Abbott, F. Acernese, K. Ackley, C. Adams, T. Adams, P. Addesso, R. X. Adhikari, V. B. Adya, *et al.*, "Search for subsolar-mass ultracompact binaries in advanced ligos first observing run," *Physical review letters*, vol. 121, no. 23, p. 231103, 2018.

[18] B. P. Abbott, R. Abbott, T. Abbott, S. Abraham, F. Acernese, K. Ackley, C. Adams, R. X. Adhikari, V. Adya, C. Affeldt, *et al.*, "Search for subsolar mass ultracompact binaries in advanced ligos second observing run," *Physical review letters*, vol. 123, no. 16, p. 161102, 2019.

ACADEMIC VITA - PHOEBE K. MCCLINCY

EDUCATION

- ***The Pennsylvania State University – University Park, PA*** **2017-2021**
  - B.S. Astronomy and Astrophysics, Minors in Physics and Mathematics
  - Expected graduation May 2021
  - **Schreyer Honors Scholar** – Merit-based scholarship and academic college for Honors students; ~5% of university student body
  - **Millennium Scholar** – Merit-based full-scholarship program designed to prepare underrepresented students for pursuit of graduate degrees in STEM; ~0.5% of university student body

RESEARCH EXPERIENCE

- ***Pennsylvania State University, Department of Physics*** **2017-Present**
  - Constraining primordial black holes as a component of dark matter with LIGO
  - Developing efficient searches for sub-solar mass compact objects with LIGO
- ***California Institute of Technology, LIGO SURF Program*** **2019**
  - Analyzing simulated populations of black holes using Bayesian statistics with LIGO
  - Inferring the underlying event rate distribution of black holes and its relation to mass and redshift with LIGO

PUBLICATIONS

- Position on LIGO Scientific Collaboration authors list as of August 2020
- LIGO Scientific Collaboration & Virgo Collaboration. (2019). *Search for subsolar mass ultracompact binaries in Advanced LIGO's second observing run.* Physical Review Letters, 123(16), 161102.
- Magee, R., Deutsch, A. S., McClincy, P., Hanna, C., et al. (2018). *Methods for the detection of gravitational waves from subsolar mass ultracompact binaries*. Physical Review D, 98(10), 103024.

AWARDS

- ***Max Planck Institute for Gravitational Physics, Summer REU*** **2020**
  - Acceptance to ten-week international REU opportunity fully funded by the University of Florida; postponed until Summer 2021 due to COVID-19
- ***Penn State University Erickson Discovery Grant*** **2018**
  - Awarded through a competitive proposal process to perform independent undergraduate research during the summer; funded current Penn State research project
- ***Penn State Millennium Scholars Program*** **2017-Present**
  - Awarded every semester; merit-based full funding for university tuition, room, and board
- ***Pennsylvania Automotive Association Community Service Scholarship*** **2017-Present**
  - Awarded each semester for excellence in community service

CONFERENCES AND PRESENTATIONS

- *"Searches for sub-solar mass ultracompact objects with Advanced LIGO."* American Physical Society National Mentoring Community Conference. Virtual. Talk. 19 February 2021.
- American Physical Society Conference for Undergraduate Women in Physics. Virtual. Attendee. 21-23 January 2021.
- *"Proposed searches for sub-solar mass ultracompact objects with Advanced LIGO."* American Physical Society Virtual April Meeting. Talk. 18-21 April 2020.
- Society for Advancement of Chicanos/Hispanics and Native Americans in Science Conference. Honolulu, HI. Attendee. 31 October-2 November 2019.
- *"Searches for sub-solar mass ultracompact objects with Advanced LIGO."* Penn State Fall Undergraduate Research Exhibition. University Park, PA. Poster. 26 September 2019.
- "*Discovering the underlying distributions of blackhole populations.*" Caltech SURF Seminar Day. California Institute of Technology, Pasadena, California. Talk. 22 August 2019.
- *"An efficient search for gravitational waves from primordial black holes."* Penn State Spring Undergraduate Research Exhibition. University Park, PA. Poster. 17 April 2019.
- *"Searches for sub-solar mass ultracompact objects with Advanced LIGO."* American Physical Society April Meeting. Denver, Colorado. Talk. 15 April 2019.
- *"An efficient search for gravitational waves from primordial black holes."* American Physical Society Bridge Program and National Mentoring Community Conference. Stanford University, Palo Alto, California. Poster. 17 November 2018.

RESEARCH SKILLS

- Computational skills: Python (proficient), Unix (proficient), HTML/CSS (proficient), Git (proficient), Wolfram (proficient), R (intermediate), JavaScript (basic), Matlab (basic)
- Signal processing (intermediate)
- Bayesian inference (intermediate)

TEACHING EXPERIENCE

- ***Department of Physics, Penn State*** **2019-Present**
  - Physics 419: Theoretical Mechanics - *Learning Assistant*
  - Physics 237: Introduction to Modern Physics - *Learning Assistant*
- ***Department of Mathematics, Penn State*** **2020**
  - Math 141: Calculus with Analytic Geometry II - *Learning Assistant*
- ***Millennium Scholars Program, Penn State*** **2018-Present**
  - Astronomy 292: Astronomy of the Distant Universe - *Tutor*
  - Math 140/141: Calculus with Analytic Geometry I/II - *Tutor*
  - Physics 211: General Physics, Mechanics - *Tutor*

COMMUNITY ENGAGEMENT

- ***Undergraduate Research Ambassadors*** *- Ambassador, Mentor* **2020-Present**
    - Represents Penn State as an undergraduate researcher via the university Office of Undergraduate Research and Fellowships Mentoring
    - Holds weekly advising office hours with the intention of mentoring underclassmen interested in pursuing undergraduate research
    - Attends alumni events, recruiting events, and student panels to speak about Penn State undergraduate research experience and opportunities
- ***Penn State Dance MaraTHON*** *- Technology Captain* **2020-Present**
    - Serves as a committee captain for THON, the world's largest student-run philanthropy
    - Writes backend and frontend code for Dash, the online management system for THON events
- ***Schreyer Institute for Teaching Excellence*** *- Student Reviewer* **2020-2021**
    - Serves on the review board for faculty awards, including the George W. Atherton Award for Excellence in Teaching and Milton S. Eisenhower Award for Distinguished Teaching
- ***Science LionPride*** *- College Representative* **2020-Present**
    - Serves as a tour guide for prospective students in Penn State's Eberly College of Science
    - Attends and speaks at prospective student events such as Accepted Student Days
    - Represents the Eberly College of Science at alumni events
- ***Millennium Society*** *- President, Primary THON Chair* **2018-2020**
    - Planned and coordinated philanthropic experiences on the local level for students in Millennium Scholars, including participating in the Penn State Dance MaraTHON, pairing with a local literacy council, working with the Climate Reality Project, and participating in science outreach projects for youths with the College of Science
- ***Society of Physics Students*** *- Member* **2017-Present**
    - Participates in leadership, networking, and professional development activities related to the field of physics
    - Maintains membership in the American Physical Society (APS) and American Astronomical Society (AAS)